European Journal of Technique

journal homepage: https://dergipark.org.tr/en/pub/ejt

Vol.14, No.1, 2024

Research Article

Frame Error Rate Approximations in Coded LoRa Systems

Rıfat Volkan Şenyuva[1*]

[1*]Maltepe University, Electrical-Electronics Engineering Department, 34857, Maltepe, Istanbul, Turkey. (e-mail: rifatvolkansenyuva@maltepe.edu.tr).

ARTICLE INFO

Received: Dec., 05. 2023
Revised: Mar., 26. 2024
Accepted: Mar., 27. 2024

Keywords:
Frame Error Rate
Hamming Coding
LoRa
Internet of Things (IoT)

Corresponding author: *Rıfat Volkan Şenyuva*

ISSN: *2536-5010* | e-ISSN: *2536-5134*

DOI: https://doi.org/10.36222/ejt.1400982

ABSTRACT

In this study, we consider the approximations for calculating the frame error rate (FER) of a communication system using the coded low power long range (LoRa) modulation for the additive white Gaussian noise (AWGN) channel. The discrete-time baseband model of the LoRa communication system encompasses the (7,4) Hamming encoder, a diagonal interleaver, a Gray encoder, and the LoRa baseband modulator. Two FER approximations using a tighter uncoded symbol error rate (SER) bound are derived. The derived approximations are compared against the numerical evaluation of the FER in Monte Carlo trials and the approximations proposed by Afisiadis *et al*. Numerical results show that the proposed FER approximations are closer to the Monte Carlo trials.

1. INTRODUCTION

In this paper we address the problem of calculating the frame error rate (FER) of the low power long range (LoRa) systems for the additive white Gaussian noise (AWGN) channel with Hamming codes which are specific linear block codes. Due to emerging Internet of Things (IoT) applications, the transmission of shorter data units, that is shorter frames, using short to medium-length linear block codes have gained renewed interest within the information theory community [1-2]. Thus, developing tighter bounds on the achievable performance via the best error correcting codes is an important research topic.

This paper focuses on the FER of a single user in a coded LoRa system using (7,4) Hamming codes. The computational complexity of calculating the exact FER of the coded LoRa systems for practical signal dimensions and constellation sizes is very high due to the involvement of combinatorics. Several approaches proposed in [3-5] tackle this problem. While [3] and [4] analyze the FER and bit error rate (BER) of a single user respectively, [5] investigates both BER and FER of the successive interference cancellation method proposed for two interfering users. Instead of the symbol error rate (SER) bound of [6] used in [3], we adapt the SER bound proposed for Rician fading channels in [7] to the AWGN channel and then employ it in the FER approximations. The proposed BER expression of [4] involves combinatorics without any advantage computational complexity-wise and does not investigate the FER. The setup of [5] differs from our single-user setup due to the collision of two users, and the performance results of [5] are empirical. We present our numerical results using the normalized signal-to-noise ratio (SNR) defined the SNR per information bit for the power-limited LoRa modulation.

The summary of this paper's contributions is as follows:

- We developed two FER approximations. These are closer to the Monte Carlo results than those in [3].
- We use a tighter SER bound without the high SNR assumption.
- The numerical results are given against the normalized SNR, which is valid for the power-limited LoRa modulation.

The remaining parts of this paper are organized as: the literature review is in Section 2. The transceiver chain and the frame structure along with demodulation and Hamming decoding of LoRa is introduced in Section 3. Then the frame error rate approximations are derived using tighter bit error rate bound in Section 4. The numerical evaluations of the frame error rate approximations are compared in Section 5. Finally, Section 6 reports the conclusions.

2. LITERATURE REVIEW

IoT is a new communication perspective where billions of interconnected devices such as sensors, actuators are envisioned to be integrated into the same network and the Internet through wireless links. IoT has many applications including smart home systems [8-9], improved security [10], smart metering, logistics, localization, tracking, health monitoring, smart farming, and environment monitoring [11-12]. Since most of the devices within this massive network are resource constrained and have low power, the wireless communication between these devices must require new specialized protocols which are investigated under the machine-type communications (MTC). All the seven layers including the physical layer up to the application layer of the open systems interconnection (OSI) reference communication model must be covered by these new specialized protocols. Amongst the viable solutions for the implementation of the IoT networks, the low-power wide-area networks (LPWANs) is becoming a rising substitute for the multihop short-range transmission technologies such as ZigBee and Bluetooth or the wireless cellular standards like the Third Generation Partnership Project (3GPP) and Long Term Evolution (LTE). LPWANs use the unlicensed industrial, scientific, and medical (ISM) frequency bands of 2.4 GHz, 868/915 MHz, 433 MHz, and 169 MHz [11-12]. The physical layer design of the LPWAN devices allow them to have rural area ranges between 10-15 km and urban area ranges between 2-5 km. The tradeoff for having these cellular-like coverage ranges is the significantly reduced data rate of LPWAN devices compared to Zigbee and Bluetooth [11-12].

One of the solutions used by the LPWANs for designing the physical layer is LoRa. LoRa is an M-ary digital modulation technique using chirp spread spectrum (CSS). LoRa employs the chirp waveforms for baseband modulation. The instantaneous frequency of the chirp waveforms is linearly increased within the symbol interval. The number of samples obtained in the output of the LoRa baseband demodulator at the end of each symbol interval depends on the spreading factor (SF). The coverage range of LoRa can be extended by increasing the SF, but the data rate is reduced [13-14].

Although the data rate can be increased by decreasing the SF and so the coverage range, it is still limited for many IoT applications such as smart homes/buildings, image transmission, and indoor IoT [15]. Thus, there is significant ongoing research on increasing the data rate and analyzing the achievable performance of the LoRa systems. It is shown that the data rate can be increased by modifying the nominal LoRa modulation proposed in the literature such as the interleaved chirp spreading (ICS) LoRa [16], the slope-shift keying (SSK) LoRa [17], and the frequency-bin-index (FBI) LoRa [15]. [18] compare the modified LoRa modulations with no coding applied and focuses on the differences in the spectral efficiency and the demodulator complexity amongst the modulations. The bounds proposed in [4,6,19-20] for the SER of the uncoded LoRa modulation use the AWGN channel model. The performance of the uncoded LoRa under Rayleigh and Rician fading channels has been investigated by [6-7,21]. The error rate for the uncoded LoRa with another interfering terminal using the same SF is analyzed in [19-20]. The expressions for calculating the BER and the FER of the coded LoRa modulation are given for the AWGN channel in [4] and [3] respectively.

3. SYSTEM MODEL

The physical layer of LoRa systems is explained in this section. The transceiver chain along with the structure of the frames used in LoRa systems is given in Figure 1. LoRa systems transmit data using the frame structure [3,5,14] shown in Figure 1. The preamble part of the frame consists of several upchirp symbols, and 4.25 symbols used as frame delimiters for synchronization. The header has the frame information such as its length, the coding rate, the cyclic redundancy check (CRC) and the checksum. The data is contained in the payload and the frame rate approximations are given for the payload part of the frame [3,5,14].

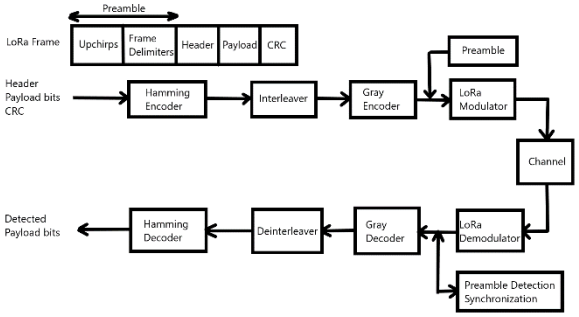

Figure 1. LoRa frame structure and transceiver chain

As it can be observed from Figure 1, the transmitter of the LoRa transceiver chain start with bit level operations including Hamming encoding, interleaving, and Gray encoding. Then LoRa modulation is used to convert Gray encoded bits into symbols and then into passband signals suitable for transmission. At the receiver chain the preamble part of the incoming signal is used for synchronization first before demodulation. Then the demodulated LoRa symbols are applied to Gray decoder, deinterleaver, and Hamming decoder in order to detect the payload bits.

2.1. LoRa Modulation and Demodulation

LoRa is an M-ary digital modulation scheme. The SF-length tuples, $(b_0, \dots, b_{\mathrm{SF}-1})$, of information bits are converted into M-dimensional signal samples, $\mathbf{a}_m = \left[a_{m,0}, \dots, a_{m,M-1}\right]^{\mathrm{T}} \in \mathcal{A}$, from the constellation $\mathcal{A} = \{\mathbf{a}_0, \dots, \mathbf{a}_{M-1}\}$ at every symbol interval, T_{symbol}, by the encoder [7]. The signal dimension, M, is equal to $M = 2^{\mathrm{SF}}$ where SF can take integer values from SF$\in\{7, \dots, 12\}$. Each symbol in the LoRa constellation, $\mathbf{a}_m$, has M samples of which only one is nonzero that is

$$a_{m,l} = \begin{cases} \sqrt{E}, l = m \\ 0, \text{else.} \end{cases} \quad (1)$$

E shows the energy of the LoRa symbol in Equation (1) and the nonzero sample index is equal to $m = \sum_{j=0}^{\mathrm{SF}-1} b_j 2^j$ [7]. The baseband signal of the LoRa modulation is written in terms of the symbols as follows

$$x_m(t) = \sum_{l=0}^{M-1} a_{m,l}\phi_l(t), \quad 0 \le t \le T_{\mathrm{symbol}} \quad (2)$$

The frequency shifted chirp waveform, $\phi_l(t)$, in Equation (2) is

$$\phi_l(t) = \exp\left\{i2\pi Wt\left[\frac{l}{M} - \frac{1}{2} + \frac{Wt}{2M} - u\left(t - \frac{M-l}{W}\right)\right]\right\} \quad (3)$$

where the chirp waveform has bandwidth W and the unit step function are shown as $u(t)$ [7,13]. Then the baseband waveform in Equation (3) is modulated to passband and the signal received at the demodulator becomes [7]

$$Y(t) = 2\Re\{[x_m(t) + N(t)]e^{i2\pi f_c t}\}, \quad 0 \le t \le T_{\text{symbol}} \quad (4)$$

In Equation (4), $\Re(\cdot)$ takes the real part of its complex argument and the additive baseband noise process, $N(t)$, is white Gaussian with its single-sided spectral density given as N_0. The sub-GHz ISM band, 863-870 MHz band, is allocated for the LoRa carrier frequencies, f_c, in Europe. The received signal in Equation (4) is first passed through the Hilbert filter and the output of the filter multiplied with the complex carrier yields the baseband signal. For the sampling interval of $T_{\text{sampling}} = 1/W$ the discrete-time baseband signal samples are

$$Y[n] = x_m[n] + N[n], \quad n = 0, \dots, M-1 \quad (5)$$

where $M = WT_{\text{symbol}}$ [7]. Both the baseband noise samples and the received signal samples in Equation (5) are circularly symmetric complex Gaussian random variables described as $N[n] \sim \mathcal{CN}(0, N_0)$ and $Y[n] \sim \mathcal{CN}(x_m[n], N_0)$ respectively. The baseband LoRa samples are given as

$$x_m[n] = \sqrt{\frac{E}{M}}(-1)^n e^{i\pi n^2/M} e^{i2\pi mn/M} = x_0[n]e^{i2\pi mn/M} \quad (6)$$

where $x_0[n] = \sqrt{E/M}(-1)^n e^{i\pi n^2/M}$ is defined as the upchirp signal [7,17]. The maximum a-posteriori probability (MAP) rule gives the optimum detector for the baseband samples in Equation (5) as

$$\hat{m} = \underset{0\le\tilde{m}\le M-1}{\text{argmax}}\, f_{\mathbf{X}|\mathbf{Y}}(\mathbf{x}_m|\mathbf{y}) = \underset{0\le\tilde{m}\le M-1}{\text{argmax}}\, \ln\left[f_{\mathbf{X}|\mathbf{Y}}(\mathbf{x}_m|\mathbf{y})\right] \quad (7)$$

where $f_{\mathbf{X}|\mathbf{Y}}(\mathbf{x}_m|\mathbf{y})$ is the conditional probability density function of $\mathbf{X} = \mathbf{x}_m = (x_m[0], \dots, x_m[M-1])^{\mathrm{T}}$ given $\mathbf{Y} = \mathbf{y} = (y[0], \dots, y[M-1])^{\mathrm{T}}$ and $\ln(\cdot)$ is the natural logarithm of its argument. According to the Bayes theorem, $f_{\mathbf{X}|\mathbf{Y}}(\mathbf{x}_m|\mathbf{y})$ is equal to

$$f_{\mathbf{X}|\mathbf{Y}}(\mathbf{x}_m|\mathbf{y}) = \frac{p_{\mathbf{X}}(\mathbf{x}_m) f_{\mathbf{Y}|\mathbf{X}}(\mathbf{y}|\mathbf{x}_m)}{f_{\mathbf{Y}}(\mathbf{y})} \quad (8)$$

$$= C\exp\left[2\Re\left\{\sum_{n=0}^{M-1} y[n]x_m^*[n]\right\}\right] \quad (9)$$

where the probability mass function for m-th message signal is shown as $p_{\mathbf{X}}(\mathbf{x}_m)$ and it is equal to $p_{\mathbf{X}}(\mathbf{x}_m) = 1/M$ due to equal probability assumption and $f_{\mathbf{Y}}(\mathbf{y})$ is the marginal probability density function (PDF) of $\mathbf{Y}$ in Equation (8) [17]. The C term in Equation (9) is not explicitly given since it is independent of the message, m, and does not affect the detection rule. Plugging Equation (9) into Equation (7) yields the optimum detector

$$\hat{m} = \underset{0\le\tilde{m}\le M-1}{\text{argmax}}\, \Re\left\{\sum_{n=0}^{M-1} y[n]x_0^*[n]e^{-i2\pi\tilde{m}n/N}\right\} \quad (10)$$

$$= \underset{0\le\tilde{m}\le M-1}{\text{argmax}}\, \Re\left\{\sum_{n=0}^{M-1} \check{R}[\tilde{m}]\right\} \quad (11)$$

where $\check{R}[\tilde{m}] = \sum_{n=0}^{M-1} r[n]e^{-i2\pi\tilde{m}n/M}$ is the discrete Fourier transform (DFT) of the dechirped signal, $r[n] = y[n]x_0^*[n]$, evaluated at $\tilde{m}$-th frequency [7]. The fast Fourier transform (FFT) algorithm may calculate the DFT of the dechirped signal in $\mathcal{O}(M \log M)$ operations.

2.2. Hamming Encoding and Decoding

(n_c, k_c) Hamming codes are implemented in LoRa systems. There are 2^{k_c} codewords of length n_c in a (n_c, k_c) Hamming code. The length of the dataword and the codewords chosen in practice are $k_c = 4$ and $n_c \in \{5,6,7,8\}$ respectively [3,5,14]. This paper investigates the frame error rate approximations of the LoRa systems for the (7,4) Hamming code which can correct single-bit errors. The LoRa payload bits, $\mathbf{u} \in \{0,1\}^{k_c}$, are Hamming encoded using

$$\mathbf{c} = (\mathbf{uG})_2 \quad (12)$$

where $\mathbf{G} = [\mathbf{I}_4\ \mathbf{P}]$ is the generator matrix for the systematic (7,4) Hamming code and $(\cdot)_2$ denotes the elementwise modulo-2. $\mathbf{I}_4$ represents the identity matrix of size 4×4 and the parity matrix is given as

$$\mathbf{P} = \begin{bmatrix} 1 & 1 & 0 \\ 0 & 1 & 1 \\ 1 & 0 & 1 \\ 1 & 1 & 1 \end{bmatrix} \quad (13)$$

Error bursts can be corrected if the codewords are interleaved such that the location of errors is distributed over many codewords. To accomplish this, LoRa systems employ a diagonal interleaver which reads SF number of codewords each with length n_c and reorder them in a block of SF rows and n_c columns shown in Figure 2.

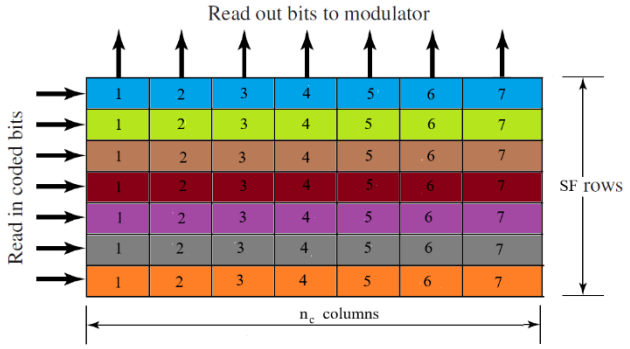

Figure 2. LoRa Interleaver for SF=7 and $n_c = 7$

Then the columns of the interleaver is Gray mapped and modulated using the LoRa signaling scheme explained in Section 2.1. Once the demodulated signal is Gray demapped in the receiver chain (Figure 1), the deinterleaver constructs an $n_c \times$ SF block structure by reordering its rows and outputs its columns. The decoding of the deinterleaved codewords is

realized by hard decision. The first step is to calculate the syndrome of the Hamming decoder input $\mathbf{v}$

$$\mathbf{s} = (\mathbf{v}\mathbf{H}^{\mathrm{T}})_2 \tag{14}$$

Then, we find the row called a coset corresponding to $\mathbf{s}$ in the standard array for the Hamming code. The first element of the corresponding coset gives the error pattern. The rows of $\mathbf{E}$ matrix in Equation (15) include all of the single-bit error patterns

$$\mathbf{E} = \begin{bmatrix} 1 & 0 & 0 & 0 & 0 & 0 & 0 \\ 0 & 1 & 0 & 0 & 0 & 0 & 0 \\ 0 & 0 & 1 & 0 & 0 & 0 & 0 \\ 0 & 0 & 0 & 1 & 0 & 0 & 0 \\ 0 & 0 & 0 & 0 & 1 & 0 & 0 \\ 0 & 0 & 0 & 0 & 0 & 1 & 0 \\ 0 & 0 & 0 & 0 & 0 & 0 & 1 \end{bmatrix} \tag{15}$$

If the corresponding coset is the l-th row of $\mathbf{E}$ shown as $\mathbf{e}_l$, then the corrected codeword can be obtained by adding it to the input vector as in

$$\hat{\mathbf{c}} = \mathbf{v} \oplus \mathbf{e}_l \tag{16}$$

where $\oplus$ is the modulo-2 elementwise vector addition.

4. FRAME ERROR RATE

The FER approximations are derived in this section. First the uncoded bit error rate is bounded and then the codeword error rate is calculated using the given bound for the uncoded bit error rate. Finally, two approximations for the FER are derived in terms of the codeword error rate.

3.1. Uncoded Bit Error Rate

The probability of a symbol error, $P_s = P(m \neq \hat{m})$, for the uncoded LoRa modulation [6] is given as

$$P_s = \sum_{k=1}^{M-1} \frac{(-1)^{k+1}}{k+1} \binom{M-1}{k} \exp\left(-\frac{k}{k+1}\frac{E}{N_0}\right) \tag{17}$$

The calculation of the binomial coefficient in Equation (17) is subject to precision errors for large M. Since the smallest M for practical LoRa systems is equal to $M = 2^7 = 128$, the calculation of Equation (17) becomes challenging. There exist several approximations in the literature for the evaluation of Equation (17) [4,6,19-21]. The upper bound proposed for Rician channels in [7] can be modified for AWGN channels by setting the mean of the channel variable to one and the variance of the channel variable to zero as in

$$P_s \approx 1 - Q_1(\alpha, \beta) + \frac{M-1}{2} e^{-E/2N_0} Q_1\left(\alpha\sqrt{2}, \beta\sqrt{2}\right) \tag{18}$$

where $Q_1(\cdot)$ is the Marcum Q function and its arguments are $\alpha = \sqrt{2E/N_0}$ and $\beta = \sqrt{2\ln(M-1)}$. The probability of a bit error can be approximated to the half of the probability of a symbol error

$$P_b = \frac{2^{\mathrm{SF}-1}}{2^{\mathrm{SF}}-1} P_s \approx \frac{P_s}{2} \tag{19}$$

3.2. Codeword Error Rate

If the output of the Hamming decoder is represented as $\hat{\mathbf{c}}$, then the probability that $\hat{\mathbf{c}}$ is not equal to the Hamming encoder output, $\mathbf{c}$, is the codeword error probability and it is given as $P_c = P(\mathbf{c} \neq \hat{\mathbf{c}})$. Since the (7,4) Hamming decoder is capable of correcting only the single-bit errors, the event of a codeword error occurs when there are at least two bits in error that is

$$P_c = P(\{w_H(\mathbf{v} - \mathbf{c}) \geq 2\}) \tag{20}$$

where $w_H(\mathbf{v} - \mathbf{c})$ shows the Hamming distance, the number of ones in the difference of $\mathbf{v}$ and $\mathbf{c}$. The bit errors at the Hamming decoder input, $\mathbf{v}_j$, are independent and identically distributed with Equation (19). The codeword error probability from Equation (20) can be calculated as

$$P_c = 1 - \left[(1-P_b)^{n_c} + \binom{n_c}{1} P_b (1-P_b)^{n_c-1}\right] \tag{21}$$

3.3. Frame Error Rate

We assume that a LoRa frame has N_p payload symbols. Choosing N_p as an integer multiple of the codeword length, n_c, results in $N_c = N_p \mathrm{SF}/n_c$ number of codewords in a LoRa frame. For one block of the interleaver, the total number of transmitted codewords is equal to SF that is $\mathbf{c}_j$ for $j \in \{1, \ldots, \mathrm{SF}\}$, and they are shown as $\mathbf{C}_{\mathrm{bl}} \in \{0,1\}^{\mathrm{SF}\times n_c}$. The block of the corrected codewords at the output of the Hamming decoder $\hat{\mathbf{c}}_j, j \in \{1, \ldots, \mathrm{SF}\}$ are given as $\hat{\mathbf{C}}_{\mathrm{bl}} \in \{0,1\}^{\mathrm{SF}\times n_c}$. For one deinterleaver block, the probability that none of the codewords are erroneously decoded is

$$P(\hat{\mathbf{C}}_{\mathrm{bl}} = \mathbf{C}_{\mathrm{bl}}) = \prod_{j=1}^{\mathrm{SF}} P(\hat{\mathbf{c}}_j = \mathbf{c}_j | \hat{\mathbf{c}}_1 = \mathbf{c}_1, \ldots, \hat{\mathbf{c}}_{j-1} = \mathbf{c}_{j-1}) \tag{22}$$

The probability that the last j-th codeword is erroneously decoded given that all the decoding's for the previous $j-1$ codewords are error free is given as

$$P_c^{(j)} = P\left(\hat{\mathbf{c}}_j \neq \mathbf{c}_j \middle| \hat{\mathbf{c}}_1 = \mathbf{c}_1, \ldots, \hat{\mathbf{c}}_{j-1} = \mathbf{c}_{j-1}\right) \tag{23}$$

The correct decoding probability in Equation (22) may be expressed in terms of Equation (23) as in

$$P(\hat{\mathbf{C}}_{\mathrm{bl}} = \mathbf{C}_{\mathrm{bl}}) = \prod_{j=1}^{\mathrm{SF}} (1 - P_c^{(j)}) \tag{24}$$

The FER for N_p symbols can be calculated as in

$$P\left(\hat{\mathbf{C}}_{\mathrm{pl}} \neq \mathbf{C}_{\mathrm{pl}}\right) = 1 - \left(\prod_{j=1}^{\mathrm{SF}} \left(1 - P_c^{(j)}\right)\right)^{N_p/n_c} \tag{25}$$

where $\hat{\mathbf{C}}_{\mathrm{pl}}, \mathbf{C}_{\mathrm{pl}} \in \{0,1\}^{N_c \times n_c}$ show the matrices containing the decoded and the transmitted codewords respectively and N_p/n_c is the number of interleaver blocks within the frame.

The calculation of Equation (25) is quite involved due to large number of possible error patterns inside a deinterleaver block. Straightforward removal of the conditioning in Equation (23) yields a first FER approximation as given in

$$P(\hat{\mathbf{C}}_{\text{pl}} \neq \mathbf{C}_{\text{pl}}) \approx 1-(1-P_c)^{\frac{N_p \text{SF}}{n_c}}, \quad (26)$$

which has a much lesser computational complexity compared Equation (25). Since the codewords errors within the same interleaver block are dependent, the first FER approximation in Equation (26) is a looser upper bound for the FER [3].
If the single-bit errors in Equation (23) is to be ignored, then a much tighter bound for the FER can be found. Equation 23 can be approximated to

$$P_c^{(j)} \approx P(\hat{\mathbf{c}}_j \neq \mathbf{c}_j | \mathbf{v}_1 = \mathbf{c}_1, \ldots, \mathbf{v}_{j-1} = \mathbf{c}_{j-1}) \quad (27)$$

The condition given in the codeword error probability in Equation (27) means that the error is due to the last j-th position in $\mathbf{v}_j$. To calculate Equation (27), the conditional probability of a symbol error must be given as

$$P_s^{(j)} = P(\hat{m} \neq m | \hat{b}_1 = b_1, \ldots, \hat{b}_{j-1} = b_{j-1}) \quad (28)$$

where $\hat{b}_j = b_j$ means that j-th bit of the symbol m is decoded correctly. Given that the error is in $\text{SF}-j+1$ bit locations due to Equation (27), the LoRa signal dimension parameter, M, in Equation (18) can be modified to express the conditional symbol error probability as follows

$$P_s^{(j)} \approx 1 - Q_1(\alpha, \beta^{(j)}) + \frac{M^{(j)}}{2} e^{-E/2N_0} Q_1(\alpha\sqrt{2}, \beta^{(j)}\sqrt{2}) \quad (29)$$

where $M^{(j)} = 2^{\text{SF}-j-1} - 1$ and $\beta^{(j)} = \sqrt{2\ln(M^{(j)})}$. The conditional bit error probability is going to be the half of Equation (29) that is $P_b^{(j)} = P_s^{(j)}/2$. The codeword error probability in Equation (27) can be written as

$$P_c^{(j)} \approx 1 - \left[\left(1-P_b^{(j)}\right)^{n_c} + \binom{n_c}{1} P_b^{(j)} \left(1-P_b^{(j)}\right)^{n_c-1}\right] \quad (30)$$

Rewriting the exact FER expression from Equation (25) using the new codeword error probability shown in Equation (30) yields the second FER approximation given as

$$P(\hat{\mathbf{C}}_{\text{pl}} \neq \mathbf{C}_{\text{pl}}) \approx 1 - \left(\prod_{j=1}^{\text{SF}} \left(1-P_b^{(j)}\right)^{n_c} + \binom{n_c}{1} P_b^{(j)} \left(1-P_b^{(j)}\right)^{n_c-1}\right)^{N_p/n_c} \quad (31)$$

5. NUMERICAL RESULTS

The empirical and analytical evaluations of the FER are presented against the signal energy per bit over the noise energy that is $E_b/N_0 = E/(\text{SF}N_0)$, since the AWGN channel using LoRa modulation is considered power-limited regime due to its spectral efficiency and the normalized SNR is E_b/N_0 for the power-limited regime. The numerical results are given for the (7,4) Hamming code. The LoRa frame has $N_p = 35$ payload symbols which is chosen as an integer multiple of $n_c = 7$. The numerical FER results are averaged over 10^6 LoRa frames. Figure 3 shows the numerical and the analytical evaluations using the proposed approximations for the FER of the (7,4) Hamming coded LoRa modulation using SF=7 under the AWGN channel. The (7,4) Hamming code has provided about 2 dB coding gain over the uncoded LoRa modulation. The first FER approximation in Equation (26) is looser to the numerical FER by more than 1 dB since it is derived by ignoring the conditioning in Equation (23). The second FER approximation in Equation (31) is within 1 dB away from the numerical result and so much tighter compared to the first approximation. Due to employing the tighter SER bound of [7], both proposed FER approximations are tighter than the approximations proposed in [3].

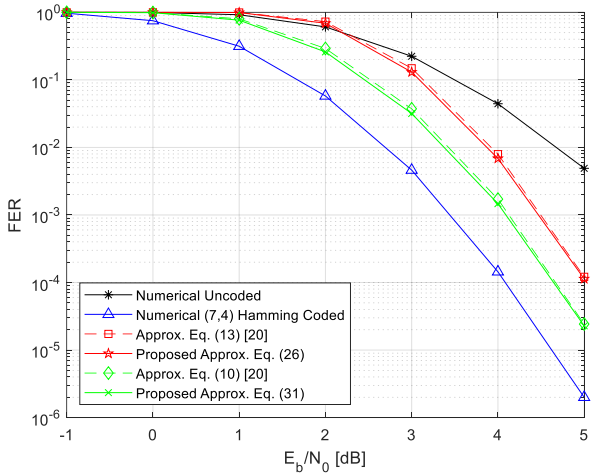

Figure 3. FER results for the (7,4) Hamming coded LoRa modulation with SF=7 under AWGN

The numerical evaluation of the first FER approximation in Equation (26) is presented for the whole range of SF values used in practice, $\text{SF}\in\{7,\ldots,12\}$, in Figure 4. The results in Figure 4 show that there is about 1.5 dB gap between SF=7 and SF=12 for FER greater than 10^{-4}. Thus, increasing the SF results in decreased FER for the coded LoRa modulation. We can see from Figure 4 that the proposed FER approximation in Equation (26) is better than the first approximation given in [3] for E_b/N_0 less than 4 dB.

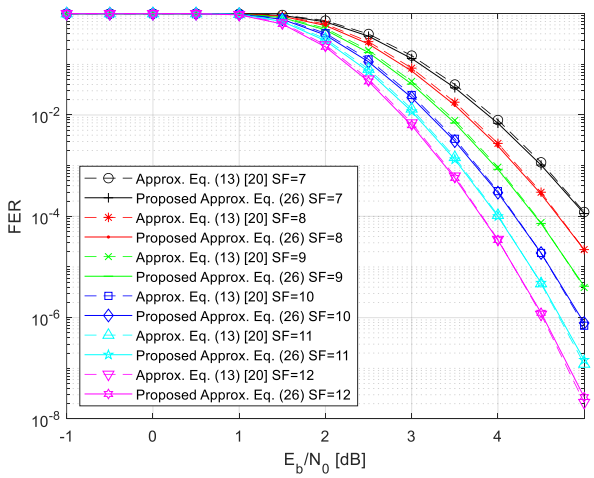

Figure 4. The FER approximation in Eq. (26) for the (7,4) Hamming coded LoRa modulation with $\text{SF}\in\{7,\ldots,12\}$ under AWGN

Figure 5 shows the results for the second FER approximation in Equation (31). Our second FER approximation slightly improves upon the corresponding approximation proposed in [20] across all SF values in the low E_b/N_0 region where E_b/N_0 less than 4 dB. For E_b/N_0 greater than 4 dB, both approximations yield the same results. The reason for this difference is while the SER bound used in the FER approximations of [3] is valid under a high SNR assumption, which does not hold in the low E_b/N_0 region, our SER bound does not rely on any SNR approximation.

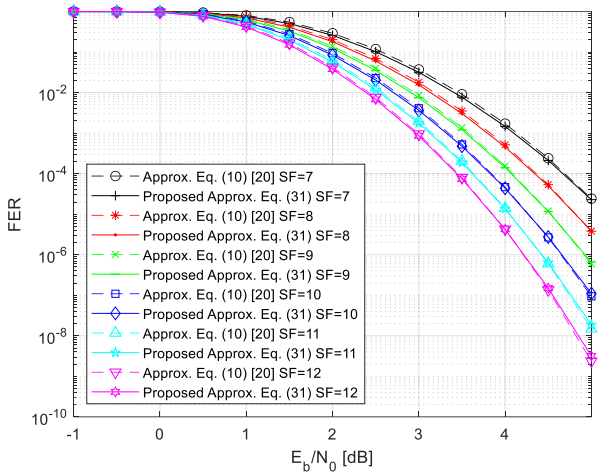

Figure 5. The FER approximation in Eq. (31) for the (7,4) Hamming coded LoRa modulation with SF∈{7, … ,12} under AWGN

6. CONCLUSION

This paper studies the approximations for calculating the FER of coded LoRa systems under the AWGN channel model. The LoRa frames of our system model pass through a (7,4) Hamming encoder, a diagonal interleaver, and a gray encoder before entering the LoRa baseband modulator. First, we derive the uncoded bit error probability of the LoRa modulation for the AWGN channel. Then, we represent the codeword error probability for the (7,4) Hamming decoder in terms of the uncoded bit error probability and give the exact FER expression. We develop two FER approximations with reduced complexity to replace the exact FER expression. We relax the conditioning between the codeword errors within the same interleaver block for the first FER approximation. As for the second FER approximation, we ignore the single-bit errors and derive a new conditional codeword error probability. We compare the proposed approximations against the numerical evaluations for varying SF. The performances of the proposed FER approximations are better than the ones proposed by Afisiadis *et al*.

REFERENCES

[1] G. Durisi, T. Koch and P. Popovski, "Toward Massive, Ultrareliable, and Low-Latency Wireless Communication With Short Packets," in *Proceedings of the IEEE*, vol. 104, no. 9, pp. 1711-1726, Sept. 2016.

[2] M. C. Coşkun et al., "Efficient error-correcting codes in the short blocklength regime," Phys. Comm., vol. 34, pp. 66-79, Jun. 2019.

[3] O. Afisiadis, A. Burg and A. Balatsoukas-Stimming, "Coded LoRa Frame Error Rate Analysis", *IEEE ICC*, Dublin, Ireland, 2020, pp. 1-6.

[4] G. Baruffa, L. Rugini, L. Germani, F. Frescura, "Error probability performance of chirp modulation in uncoded and coded LoRa systems," Digit. Signal Process., vol. 106, Nov. 2020.

[5] J. Tapparel, M. Xhonneux, D. Bol, J. Louveaux and A. Burg, "Enhancing the reliability of dense LoRaWAN networks with multiuser receivers", IEEE Open J. Commun. Soc., vol. 2, pp. 2725-2738, 2021.

[6] T. Elshabrawy and J. Robert, "Closed-Form Approximation of LoRa Modulation BER Performance," in *IEEE Comm. Letters*, vol. 22, no. 9, pp. 1778-1781, Sept. 2018.

[7] R. V. Şenyuva, "Union bounds on the symbol error probability of LoRa modulation for flat Rician block fading channels", *Phys. Comm.*, vol. 58, 2023.

[8] Z. L. OO, T. W. Lai, and A. Moe, "IoT Based Home Automation System using a REST API Architecture", *EJT*, vol. 12, no. 2, pp. 123-128, 2022.

[9] R. Daş, and T. Ababaker, "Design and Application of a Smart Home System based on Internet of Things", *EJT*, vol. 11, no. 1, pp. 34-42, 2021.

[10] F. Abdulkafi, S. Kurnaz, and F. A. Abdulkafi, "Security Improvements of Internet of Things Systems." *EJT*, vol. 10, no. 2, pp. 476 - 488, 2020.

[11] U. Raza, P. Kulkarni and M. Sooriyabandara, "Low Power Wide Area Networks: An Overview," in *IEEE Comm. Surveys & Tutorials*, vol. 19, no. 2, pp. 855-873, Secondquarter 2017.

[12] M. Centenaro, L. Vangelista, A. Zanella and M. Zorzi, "Long-range communications in unlicensed bands: the rising stars in the IoT and smart city scenarios," in *IEEE Wireless Comm.*, vol. 23, no. 5, pp. 60-67, Oct. 2016.

[13] M. Chiani and A. Elzanaty, "On the LoRa Modulation for IoT: Waveform Properties and Spectral Analysis," in *IEEE Internet Things J.*, vol. 6, no. 5, pp. 8463-8470, Oct. 2019.

[14] R. Ghanaatian, O. Afisiadis, M. Cotting and A. Burg, "Lora Digital Receiver Analysis and Implementation," *IEEE ICASSP*, Brighton, UK, 2019, pp. 1498-1502.

[15] H. Ma, Y. Fang, G. Cai, G. Han and Y. Li, "A New Frequency-Bin-Index LoRa System for High-Data-Rate Transmission: Design and Performance Analysis," in *IEEE Internet Things J.*, vol. 9, no. 14, pp. 12515-12528, July 2022.

[16] T. Elshabrawy and J. Robert, "Interleaved Chirp Spreading LoRa-Based Modulation," in *IEEE Internet Things J.*, vol. 6, no. 2, pp. 3855-3863, April 2019.

[17] M. Hanif and H. H. Nguyen, "Slope-Shift Keying LoRa-Based Modulation," in *IEEE Internet Things J.*, vol. 8, no. 1, pp. 211-221, 1 Jan.1, 2021.

[18] R. V. Şenyuva, "Comparison of LoRa-Based Modulations," IEEE SIU, Safranbolu, Turkey, 2022, pp. 1-4.

[19] O. Afisiadis, M. Cotting, A. Burg and A. Balatsoukas-Stimming, "On the Error Rate of the LoRa Modulation With Interference," in *IEEE Trans. Wireless Comm.*, vol. 19, no. 2, pp. 1292-1304, Feb. 2020.

[20] O. Afisiadis, S. Li, J. Tapparel, A. Burg and A. Balatsoukas-Stimming, "On the Advantage of Coherent LoRa Detection in the Presence of Interference," in *IEEE Internet Things J.*, vol. 8, no. 14, pp. 11581-11593, July 2021.

[21] J. Courjault, B. Vrigneau, O. Berder and M. R. Bhatnagar, "A Computable Form for LoRa Performance Estimation: Application to Ricean and Nakagami Fading," in *IEEE Access*, vol. 9, pp. 81601-81611, 2021.

BIOGRAPHIES

Rıfat Volkan Şenyuva (8p) graduated from Istanbul Technical University, Istanbul, Turkey, with dual B.Sc. degrees in control engineering (2007) and computer engineering (2008). He then continued his studies at Boğaziçi University, Istanbul, Turkey, where he received M.Sc. (2009) and Ph.D. (2016) degrees in electrical–electronics engineering. His Ph.D. dissertation was focused on sparse signal recovery algorithms. From 2016 to 2018, he worked as a researcher in NETAS Telecommunication Inc. Since 2018, he has been with the Faculty of Engineering and Natural Sciences of Maltepe University, Istanbul, Turkey, where he is an Assistant Professor at the Department of Electrical–Electronics Engineering. His current research interests include multidimensional harmonic retrieval, machine-type communications, channel estimation in reconfigurable intelligent surface based systems.